Supporting Information

Modulating the Packing of [Cu_{24}(isophthalate)$_{24}$] Cuboctahedra in a Triazole-Containing Metal-Organic Polyhedral Framework

Yong Yan,[a] Mikhail Suetin,[a] Elena Bichoutskaia,[a] Alexander J. Blake,[a] David R. Allan,[b] Sarah A. Barnett[b] and Martin Schröder*[a]

a. School of Chemistry, University of Nottingham, University Park, Nottingham NG7 2RD, UK

b. Diamond Light Source, Harwell Science and Innovation Campus, Didcot, Oxfordshire OX11 0DE.

1. Materials and General methods. Commercially available reagents were used as received without further purification. Elemental analyses (C, H, and N) were performed on a CE-440 elemental analyzer at the University of Nottingham. IR spectra were recorded in the range of 550−4000 cm^{-1} on a Nicolet is5 FT-IR spectrophotometer using the attenuated total reflectance (ATR) mode. ^{1}H NMR spectra were recorded on a Bruker DRX-300 spectrometer. Thermal gravimetric analyses (TGA) were performed under a flow of nitrogen (20 mL/min) with a heating rate of 5 °C/min using a TA SDT-600 thermogravimetric analyzer. X-ray Powder Diffraction (PXRD) measurements were carried out at room temperature on a PANalytical X'Pert PRO diffractometer using Cu-*Kα* radiation (λ = 1.5418 Å) at 40 kV, 40 mA, at a scan speed of 0.02°/s and a step size of 0.005° in 2θ.

N_2, H_2 and CO_2 Isotherms. N_2, H_2 and CO_2 isotherms were determined using an IGA gravimetric adsorption apparatus (Hiden) at the University of Nottingham in a clean ultra high vacuum system with a diaphragm and turbo pumping system. Before measurements, about 120 mg solvent-exchanged samples were loaded into the sample basket within the adsorption instrument and then degassed under dynamic vacuum at 110 °C for 12 h to obtain the fully desolvated samples. In H_2 adsorption experiments, ultra-pure plus grade H_2 (99.9995%, BOC Gases) was purified further using calcium aluminosilicate and activated carbon adsorbents to remove trace amounts of water and other impurities before introduction into the IGA system. The density of liquid H_2 at the boiling point (0.0708 g/cm^3) was used for the adsorbate buoyancy correction. The density of bulk H_2 in the buoyancy correction was calculated by the Redlich-Kwong-Soave equation of state of H_2 which is built within the IGASWIN software of the IGA system.

2. Synthesis of H_6BTTI and NOTT-122

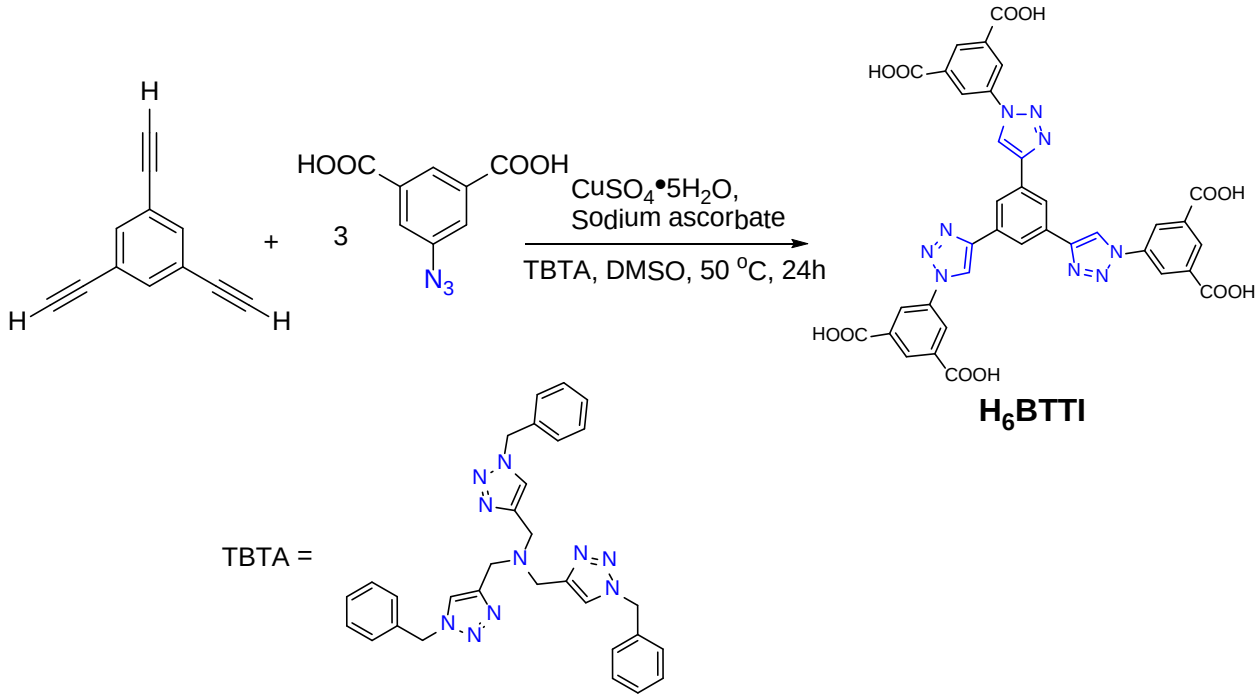

TBTA: tris[(1-benzyl-1H-1,2,3-triazol-4-yl)methyl]amine[2]

Synthesis of H_6BTTI. A mixture of 1,3,5-triethynylbenzene[1] (1.5 g, 10 mmol, 1 equiv.), 5-azidoisophthalic acid[1] (6.8 g, 33 mmol, 3.3 equiv.), sodium ascorbate (0.990 g, 5 mmol, 0.5 equiv.), TBTA[2] (372 mg, 0.7 mmol) and DMSO/H_2O (20/1, 105 mL) was degassed under Ar for 30 min. $CuSO_4$•$5H_2O$ (374 mg, 1.5 mmol) was added and the mixture stirred for 48 h at 50 °C. The mixture was treated with water and the precipitate was collected by filtration. The crude product was purified by recrystallization from DMSO/DMF to afford H_6BTTI as a white powder (6.3 g, 82 %). ^{1}H-NMR (300 MHz, DMSO-d_6): δ (ppm) = 13.601 (s, 6H, COO*H*), 9.450 (s, 3H, Ar*H*), 8.567 (s, 6H, Ar*H*), 8.402 (s, 6H, Ar*H*). MS (ESI) m/z = $[M-H]^-$ 770.1270.

Synthesis of NOTT-122, $[Cu_3(C_{36}H_{15}O_{12}N_9](H_2O)_3]$•10DMF•$10H_2O$. H_6BTTI (0.1 g, 0.13 mmol) and $Cu(NO_3)_2$•$2.5H_2O$ (0.186 g, 0.8 mmol) were mixed and dispersed in DMF/H_2O (15 mL, 5:1 v/v). HCl (2 M, 0.3 mL) was added to the mixture which was mixed thoroughly. The solution was heated without stirring using at 85 °C using an oil bath for 18 h, and a large amount of microcrystalline product precipitated. The blue-green crystalline product was separated by filtration and washed with warm DMF, and dried briefly in

air. Yield: 0.15 g (60%). Anal. Calcd (Found) for $C_{66}H_{111}Cu_3N_{19}O_{35}$: C, 41.26 (41.33); H, 5.82 (5.21); N, 13.85 (13.75)%.

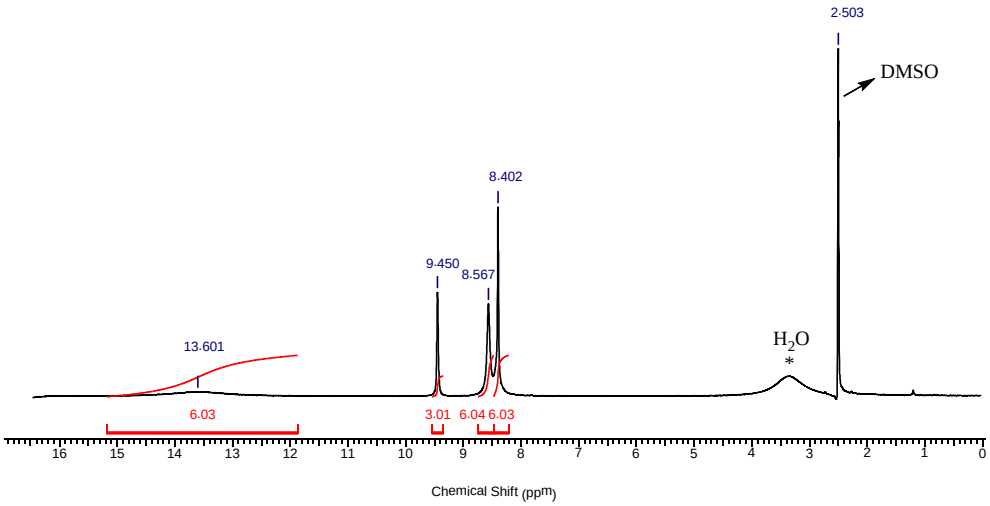

Figure S1. ^{1}H-NMR spectrum of H_6BTTI in DMSO-d_6.

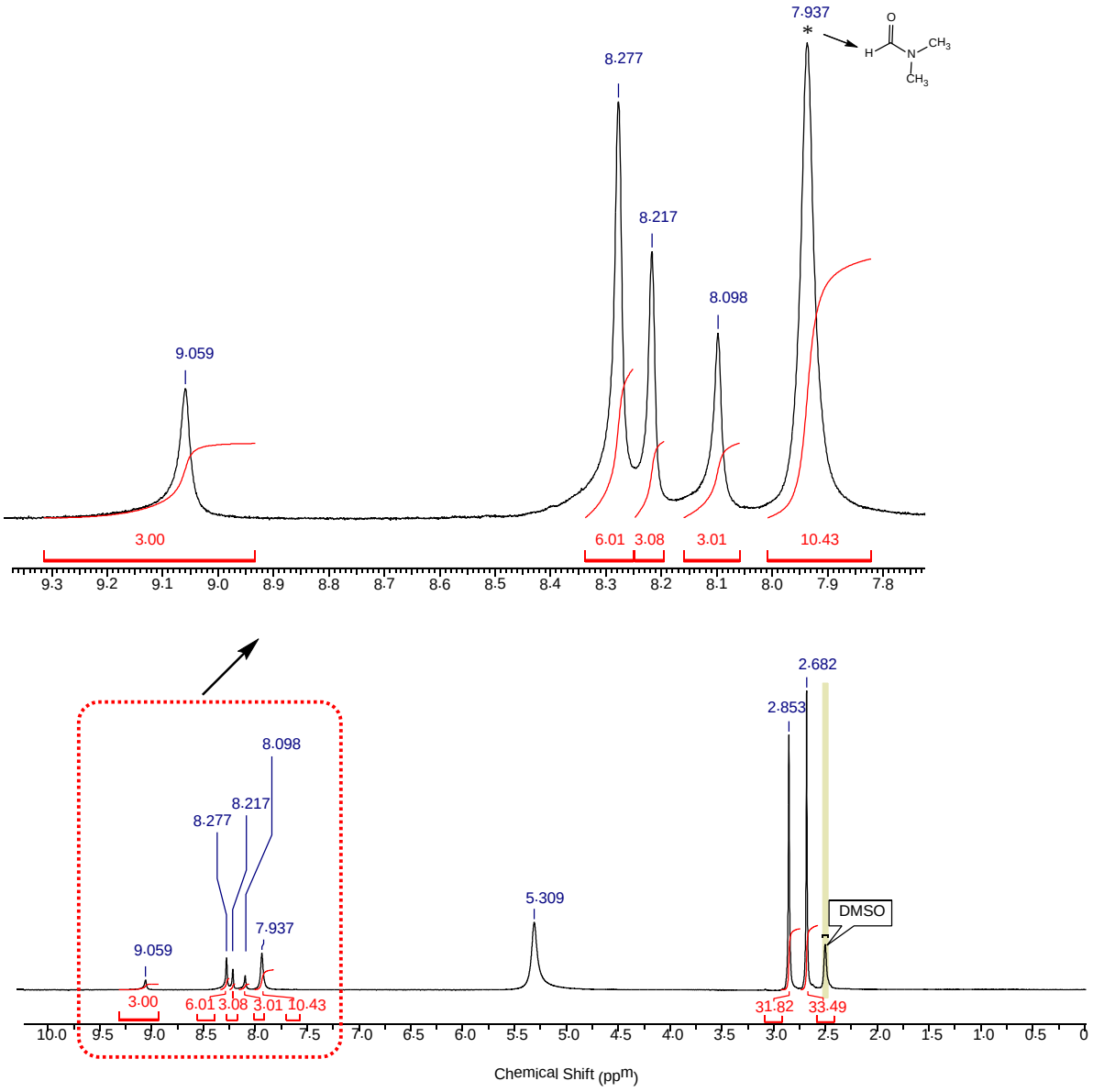

Figure S2. ^{1}H NMR spectrum of the as-synthesised NOTT-122 after digesting in DCl/DMSO-d_6 solution. Integration of the DMF proton signals gives the ratio of the DMF molecules and the $BTTI^{6-}$ unit as 10 : 1 within the formula of NOTT-122.

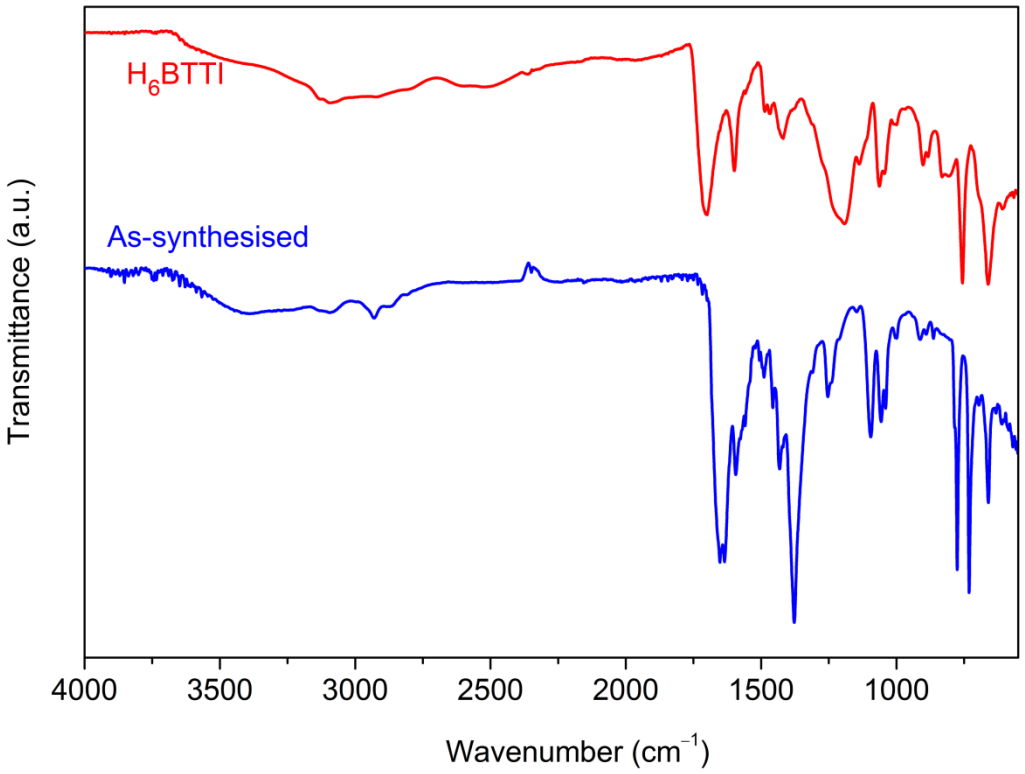

Figure S3. IR spectrum of H_6BTTI and of as-synthesised NOTT-122.

3. Single Crystal X-ray Structure Determination on NOTT-122

Single crystal diffraction data were collected on Beamline I19 of Diamond Light Source, Oxford, UK. Details of the data collection are included in the CIF. The structure was solved by direct methods and developed by difference Fourier techniques, both using the SHELXTL software package.[3] The hydrogen atoms of the ligands were placed geometrically and refined using a riding model, and the hydrogen atoms of the coordinated water molecules could not be located but are included in the formula. The unit cell volume includes a large region of disordered solvent which could not be modelled as discrete atomic sites. We therefore employed PLATON/SQUEEZE[4] to calculate the contribution of the solvent region to the diffraction and thereby produced a set of solvent-free diffraction intensities.

Table S1. Crystal data and structure refinement details for NOTT-122.

	NOTT-122
Formula	$C_{66}H_{111}Cu_3N_{19}O_{35}$
Formula weight	1921.36
Temperature	123 (2) K
Radiation type	Synchrotron
λ (Å)	0.6889
Crystal System	Tetragonal
Space Group	*I4/m*
Unit Cell Dimensions	$\alpha = \beta = \gamma = 90^o$ $a = b = 30.926(5)$ Å, c = 45.103(7) Å
Volume	43137(11) Å^3
Z	16
Density	1.183 g/cm^3
Absorption coefficient	0.663 mm^{-1}
F(000)	16112
Crystal Size	0.1 × 0.1 × 0.1 mm^3
Reflections collected	53063
Independent reflections	18798 [R_{int} = 0.0491]
Absorption correction	multi-scan
Refinement method	Full-matrix least-squares on F^2
Data / restraints / parameters	18798 / 488/ 553
GOF on F^2	1.012
Final *R* indices [$I > 2\sigma(I)$]	R_1 = 0.065, wR_2 = 0.189
Final *R* indices (all data)	R_1 = 0.081, wR_2 = 0.201
Difference Fourier map: maximum peak, minimum trough (*e* Å^{-3})	1.184, −0.554

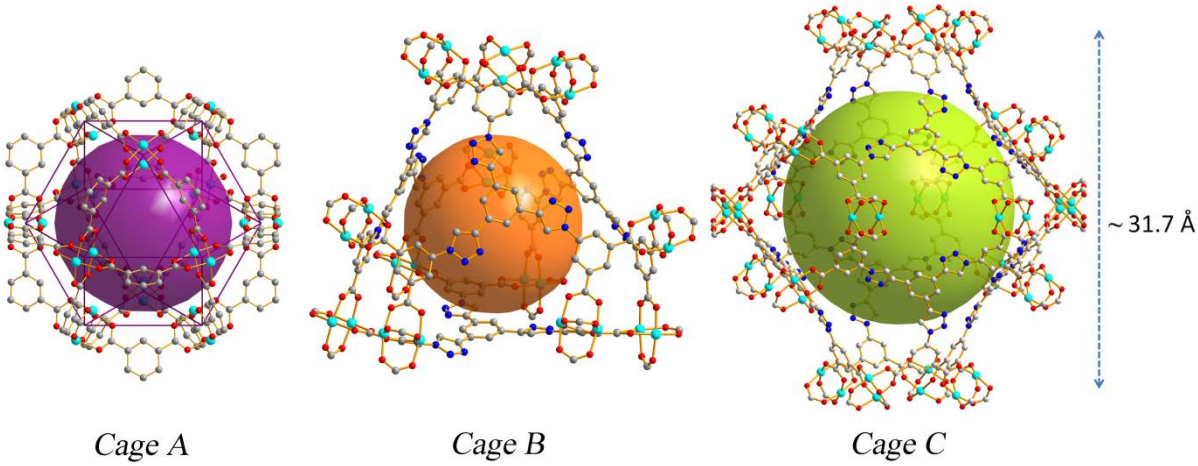

Figure S4. View of three different cages in NOTT-122.

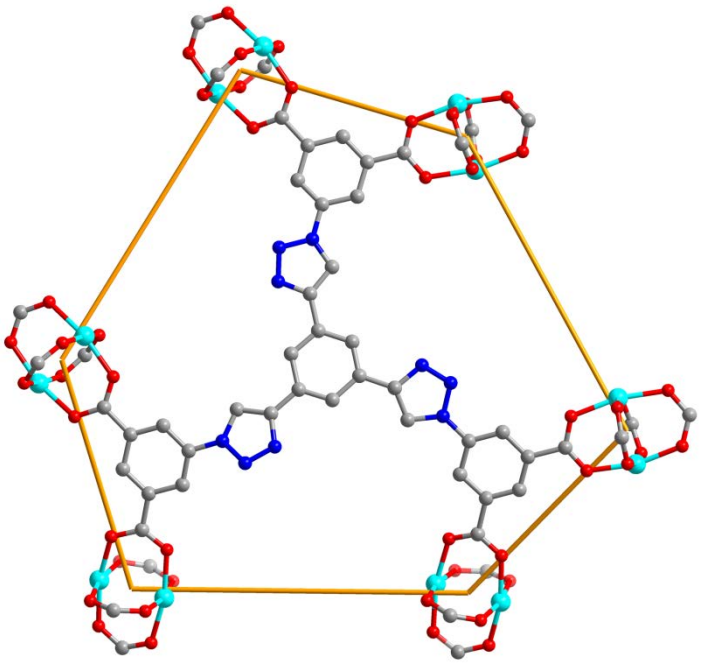

Figure S5. View of the distorted hexagonal face formed by the linker $(BTTI)^{6-}$ with $\{Cu_2(COO)_4\}$ paddlewheels in NOTT-122.

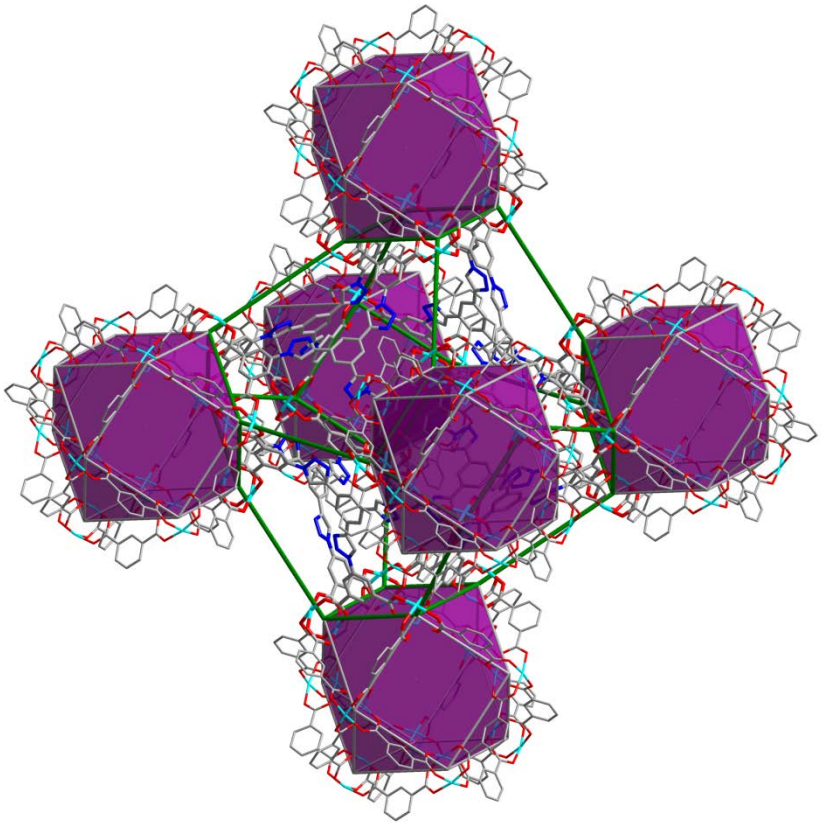

Figure S6. View of the packing of the cuboctahedra and the distorted truncated octahedra in NOTT-122.

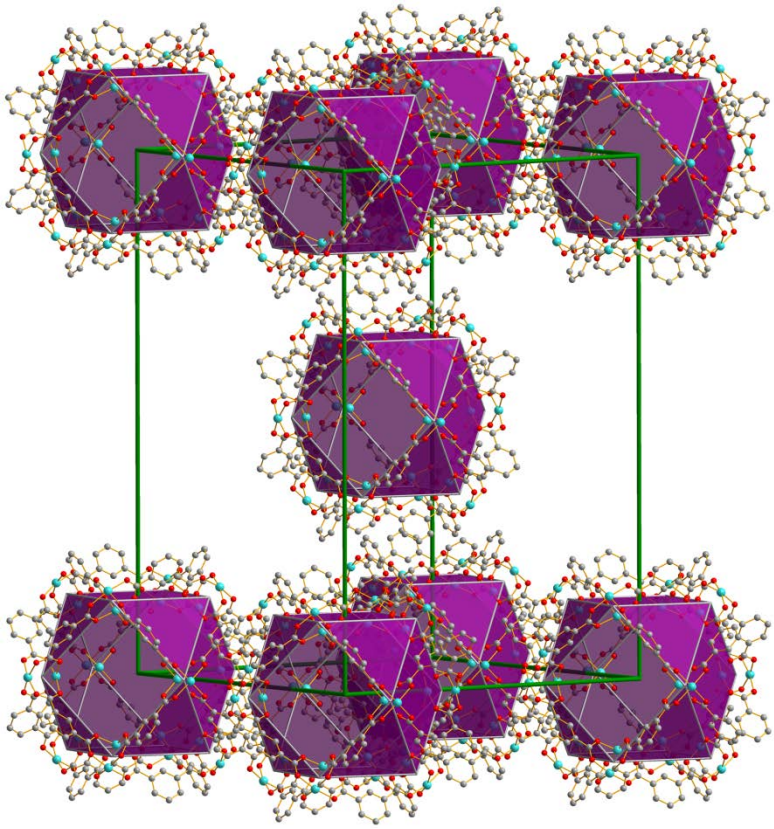

Figure S7. View of the body-centred tetragonal packing of cuboctahedra in the framework of NOTT-122.

4. TGA plot

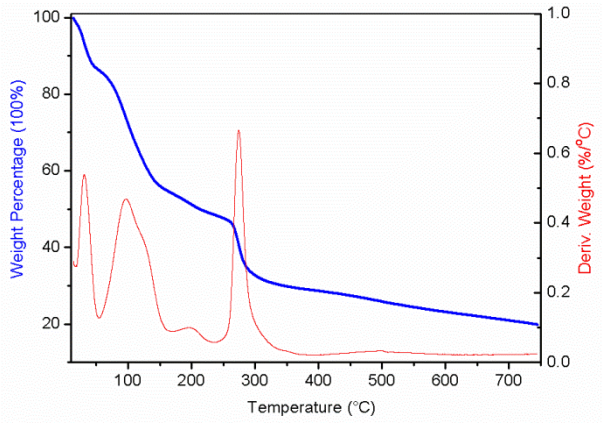

Figure S8. TGA plot of as-synthesised NOTT-122.

5. PXRD patterns

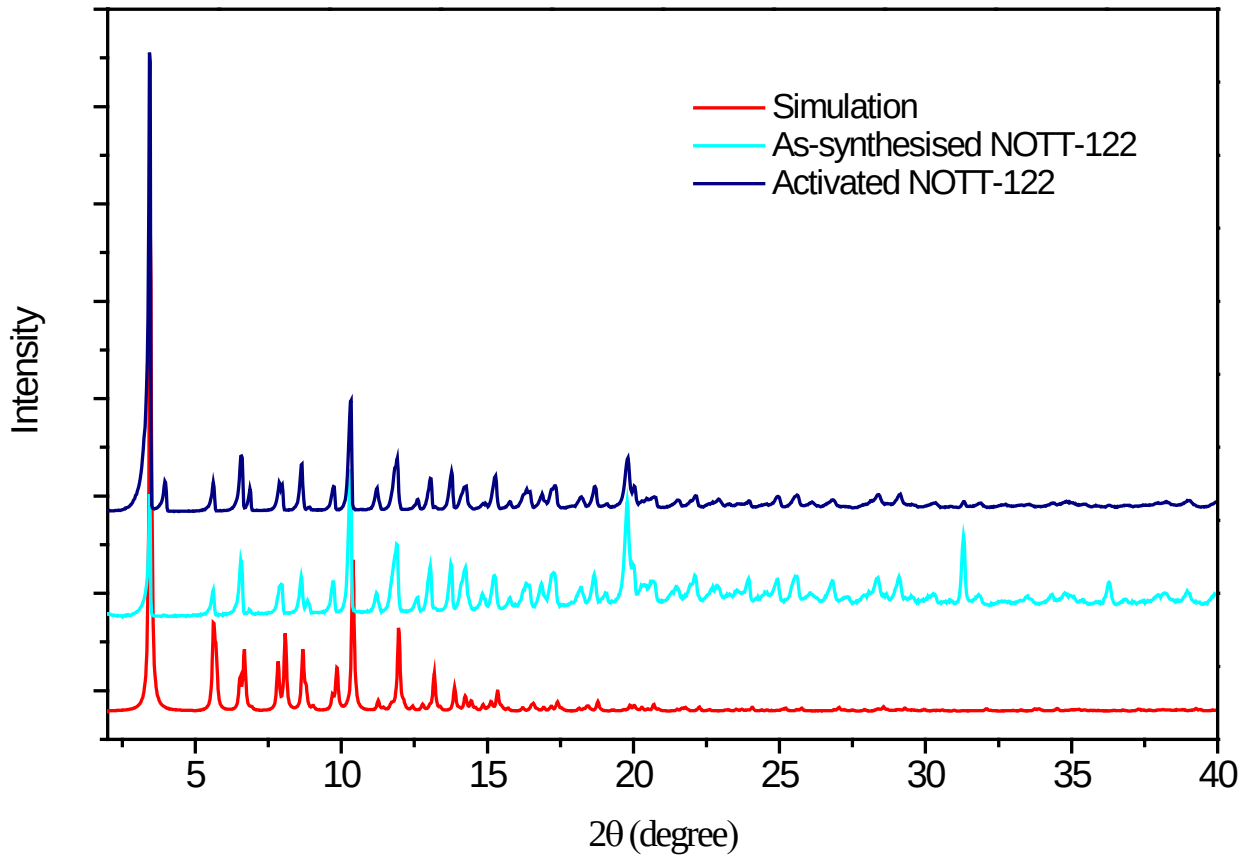

Figure S9. The PXRD patterns for NOTT-122. The activated sample was obtained by heating the acetone-exchange sample at 110 ^{o}C under dynamic vacuum for 12 h.

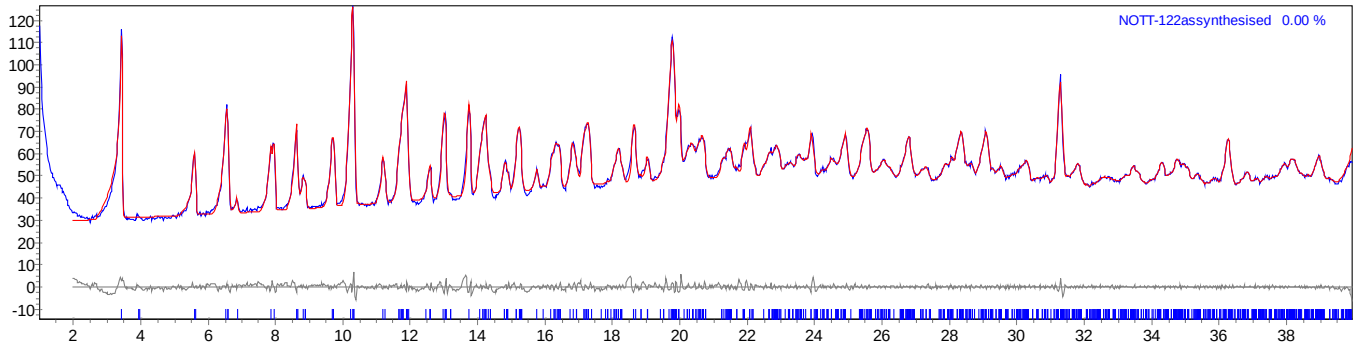

Figure S10. Le Bail fitting for the PXRD pattern of as-synthesised NOTT-122 (red: calculated; blue: observed; gray: difference; R_{wp} = 4.24%).

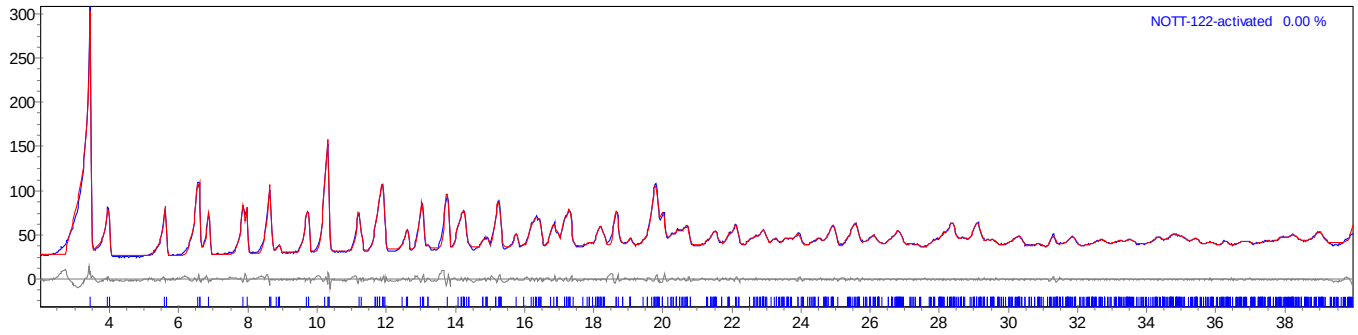

Figure S11. Le Bail fitting for the PXRD pattern of the activated NOTT-122a (R_{wp} = 7.12%).

6. BET surface area and pore size distribution

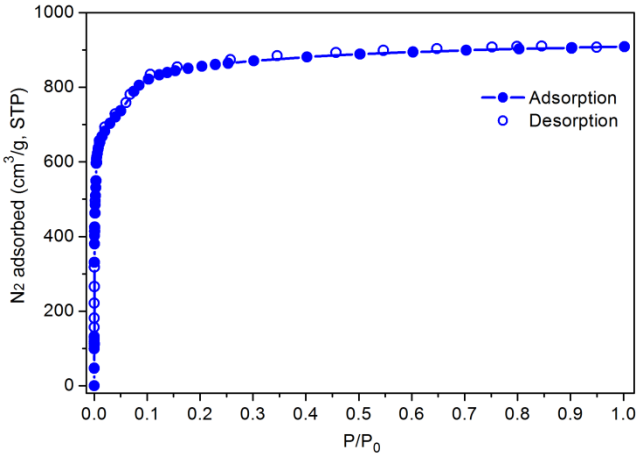

Figure S12. N_2 adsorption-desorption isotherms for NOTT-122a at 77 K.

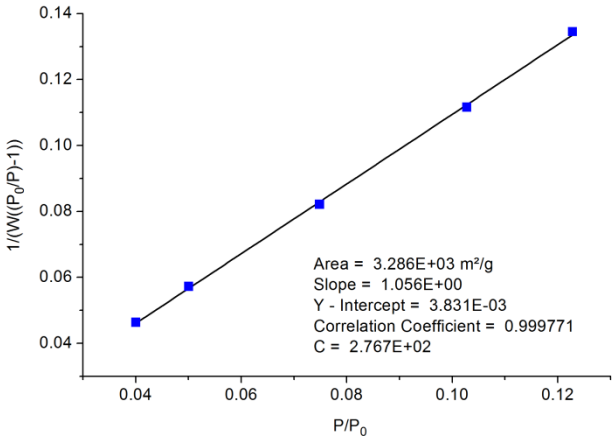

Figure S13. The BET plot derived from N_2 uptake in NOTT-122a in the range (P/P_0 = 0.04 – 0.13).

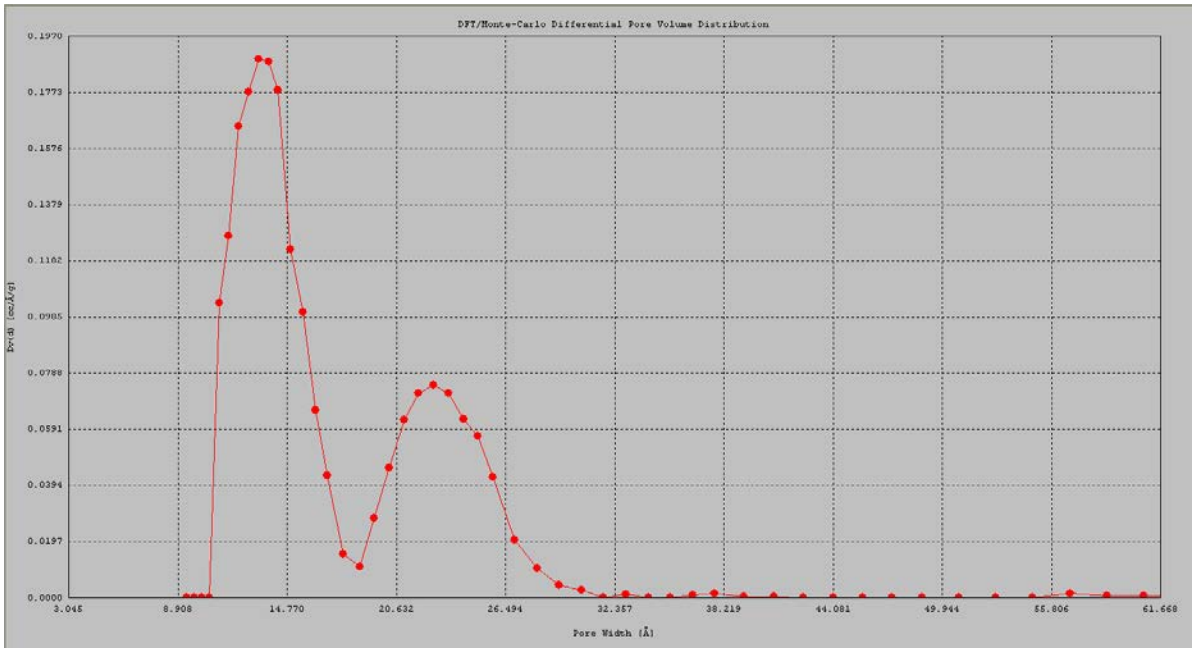

Figure S14. Pore size distribution for NOTT-122a calculated by NLDFT.

7. H_2 sorption isotherms and heats of H_2 adsorption for NOTT-122a

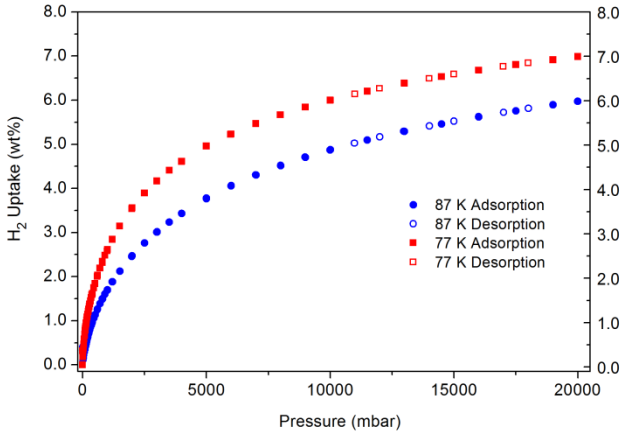

Figure S15. H_2 sorption isotherms for NOTT-122a at 77 and 87 K. wt% = 100(weight of adsorbed H_2/weight of host material).

A virial-type expression[5–7] (eq 1, virial method II) was used to fit the combined isotherm data at 77 and 87 K:

$$\ln(P) = \ln(N) + (1/T)\sum_{i=0}^{m} a_i N^i + \sum_{j=0}^{n} b_j N^j \quad (1)$$

Here, P is the pressure expressed in mbar, N is the amount adsorbed in mol/g, T is the temperature in K, a_i and b_j are Virial coefficients (temperature independent empirical parameters), and m and n represent the number of coefficients. The equation was fitted using the **R** statistical software package.[8] The values of the virial coefficients a_0 through a_m were then used to calculate the isosteric heat of adsorption using the following equation:

$$Q_{st} = -R\sum_{i=0}^{m} a_i N^i \quad (2)$$

Here, Q_{st} is the coverage-dependent isosteric heat of adsorption and R is the universal gas constant.

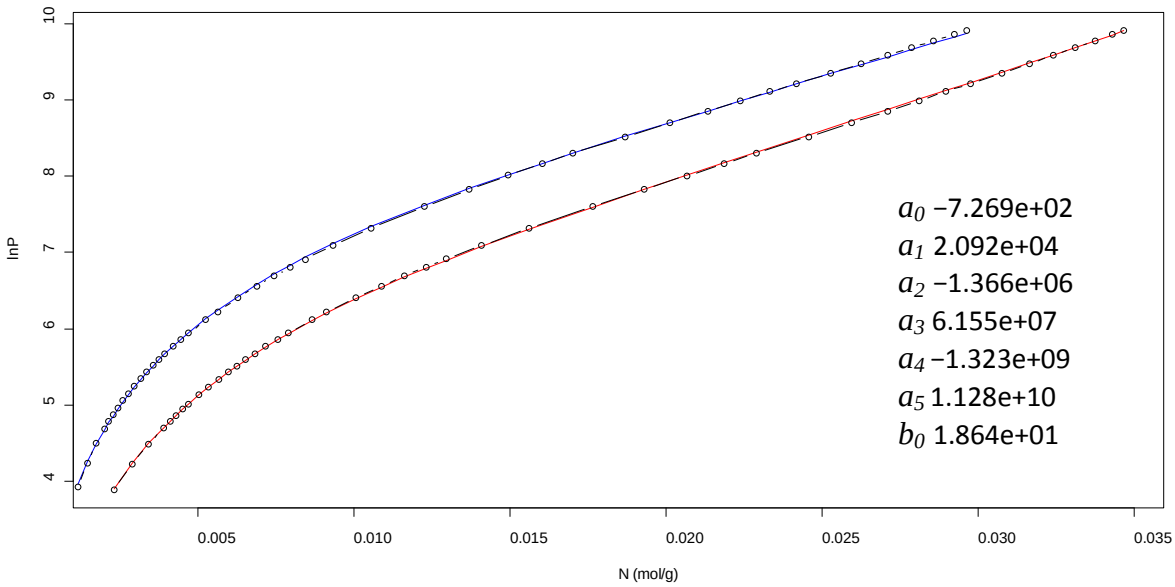

Figure S16. Virial analysis of the H_2 adsorption data for NOTT-122a (red line: 77 K; blue line, 87 K).

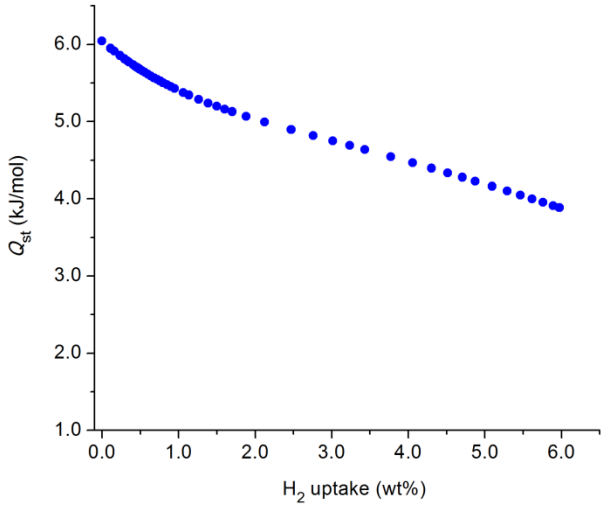

Figure S17. Heats of adsorption for H_2 in NOTT-122a.

8. Heats of adsorption for CO_2 in NOTT-122

The CO_2 adsorption isotherms at 273 and 298 K were fitted to the virial equation (eq 3, virial method I):[9–11]

$$\ln\left(\frac{n}{P}\right) = A_0 + A_1 n + A_2 n^2 + A_3 n^3 + \ldots (3)$$

where P is the pressure, n is total amount adsorbed and A_0, A_1, A_2 etc. are virial coefficients. The Henry's Law constant is given by $K_H = \exp(A_0)$. The enthalpy of adsorption at zero coverage was determined from the relationship:

$$\delta A_0 = R Q_{st}^{n=0} \delta(T^{-1}) \quad (4)$$

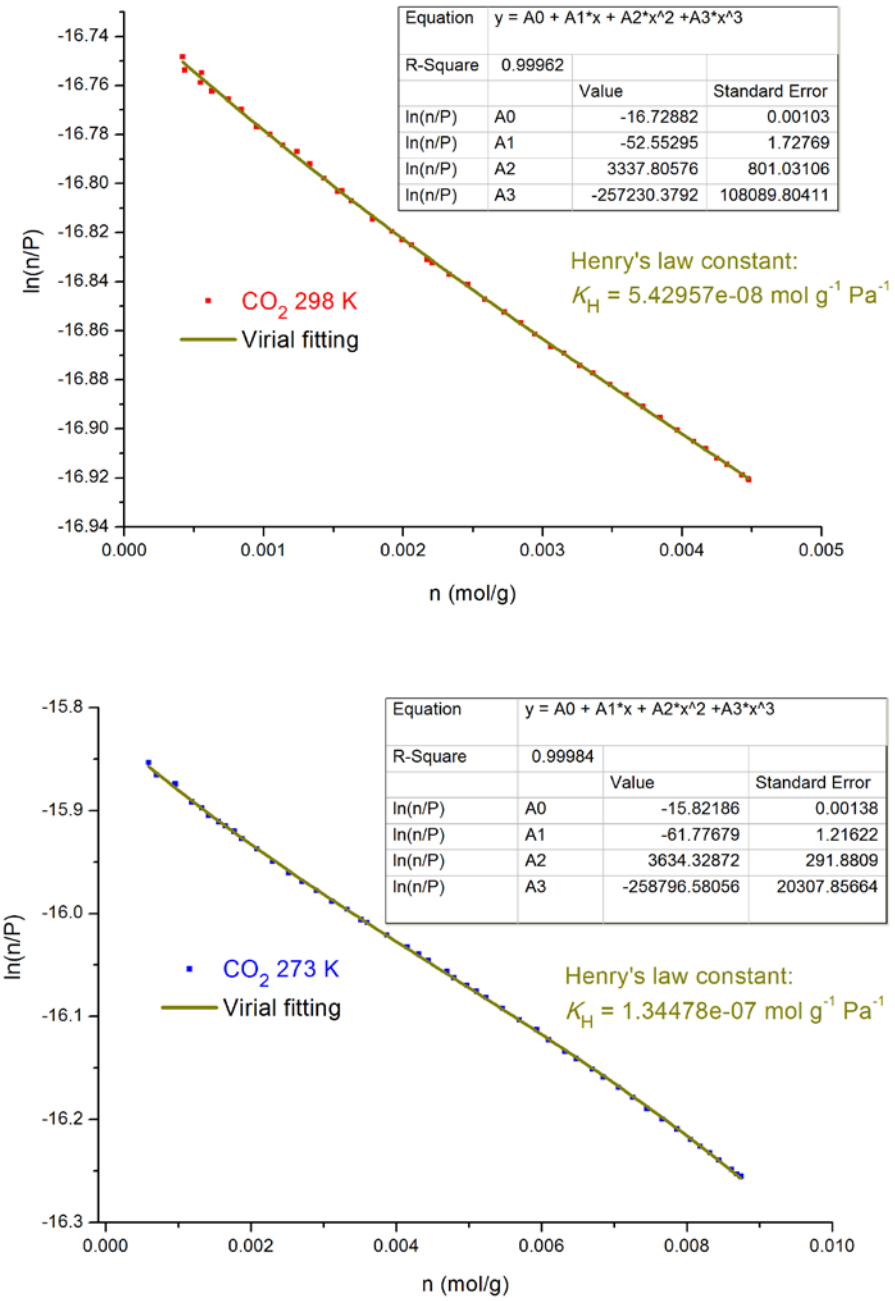

Figure S18. Virial analysis of the CO_2 isotherms for NOTT-122a at 298 and 273 K.

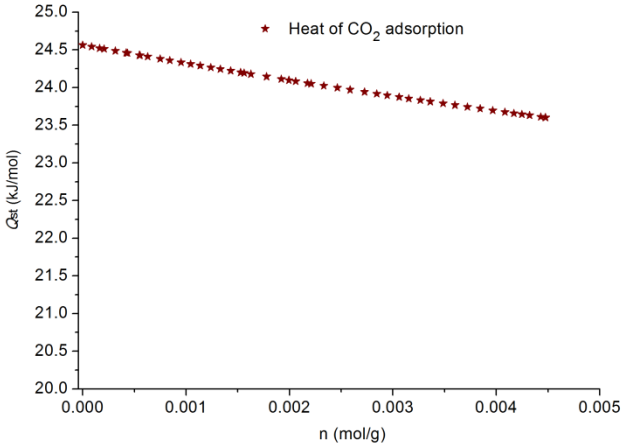

Figure S19. Heats of adsorption of CO_2 in NOTT-122a.

9. CO_2 sorption isotherm for NOTT-122 at 20 bar and 298 K

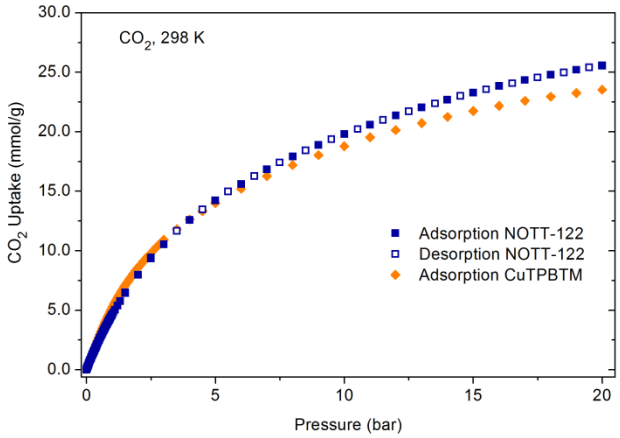

Figure S20. Comparison of the CO_2 adsorption isotherms for NOTT-122a and CuTPBTM[12] in the pressure range of 0−20 bar at 298 K.

10. CO_2/N_2 and CO_2/CH_4 Selectivities in NOTT-122a

The Henry's Law selectivity for gas component *i* over *j* at a specific temperature is calculated based on Eq. 5.

$$S_{ij} = K_{Hi}/K_{Hj} \quad (5)$$

The Henry's Law constants for N_2 and CH_4 adsorption at 298 and 273 K were calculated directly from the adsorption isotherms.

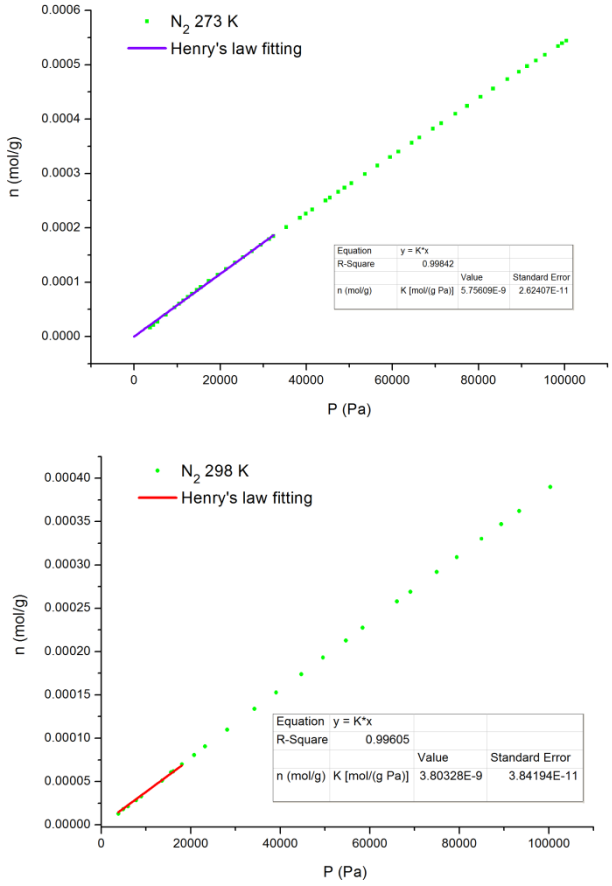

Figure S21. Fitting of the initial slope in N_2 isotherms for NOTT-122a collected at 273 and 298 K.

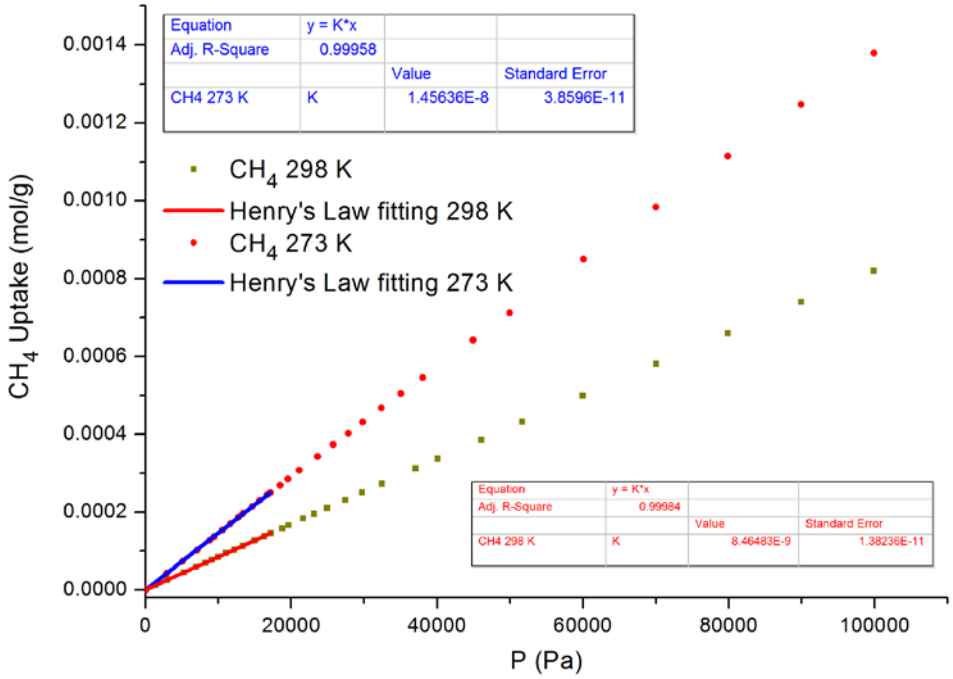

Figure S22. Fitting of the initial slope for CH_4 isotherms for NOTT-122 collected at 273 and 298 K.

11. GCMC simulations for H_2, CH_4 and CO_2 adsorption in NOTT-122a.

Grand Canonical Monte Carlo (GCMC) simulations were performed to assess the adsorption of H_2, CH_4 and CO_2 in NOTT-122a. Periodic boundary conditions were applied to a unit cell. The simulation parameters for CO_2 were taken from the TraPPE force field.[13] The CO_2 molecule was assumed to have the C−O bond length of 1.16 Å, and three charged Lennard-Jones interaction sites with the following parameters: σ_O=3.05 Å, ε_O/k_B = 79 K for oxygen atom, and σ_C = 2.80 Å and ε_C/k_B = 27 K for carbon atom. A point charge of + 0.7 was placed at the centre of mass of carbon atom and a point charge of −0.35 was placed at oxygen atom. The fugacity was calculated from the Peng-Robinson equation of state,[14] and the dispersion interactions of the framework atoms modelled by the Universal Force Field (UFF).[15] A number of simulation studies have shown that UFF can accurately predict gas adsorption in various MOFs.[16–19] The DREIDING force field[20] was employed to describe parameters of the framework in the H_2 and CH_4 sorption simulation. The framework and the gas molecules were considered to be rigid. Lennard-Jones (LJ) potential has been used to describe the Van der Waals interactions with a cut-off distance of 15.0 Å. The partial charges for atoms of the MOF have been computed using CHELPG approach, B3LYP level of density functional theory, and the 6-31G* basis set as implemented in Q-Chem quantum chemistry package.[21] The GCMC simulations were performed with MUSIC simulation

suite[22] and included 10^7 step equilibration period followed by 10^7 step production run.

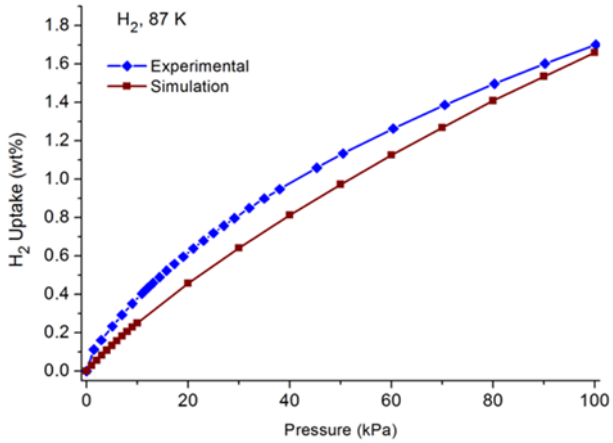

Figure S23. Comparison of the experimental and simulated H_2 adsorption isotherms for NOTT-122 at 87 K.

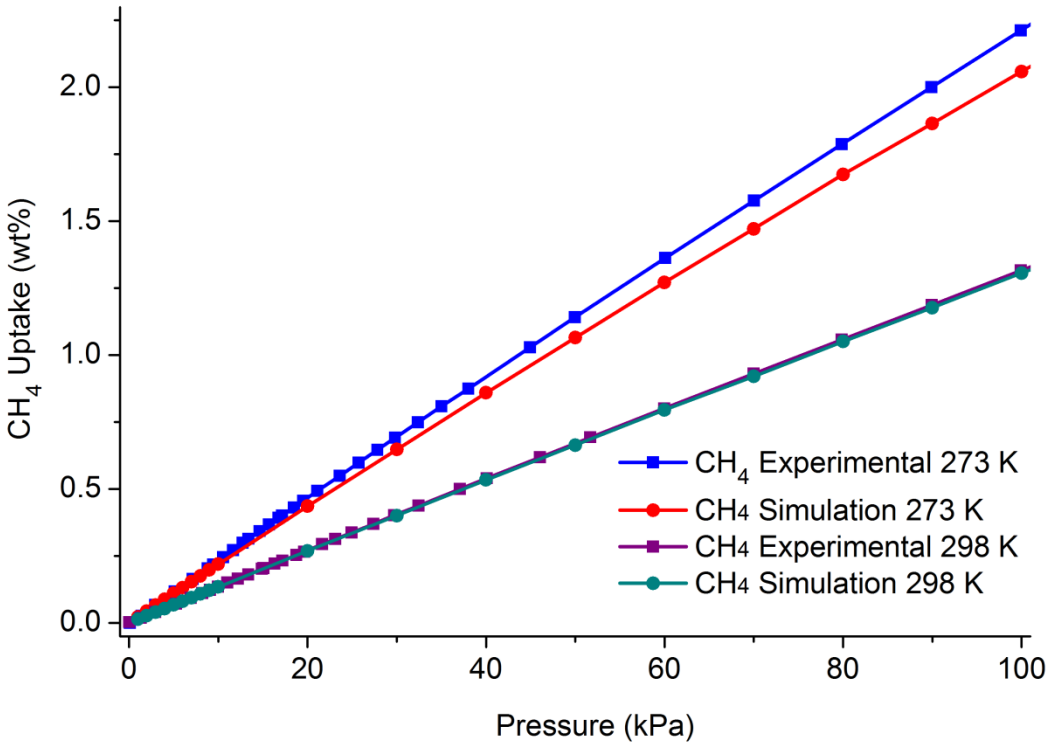

Figure S24. Comparisons of the experimental and simulated CH_4 adsorption isotherms for NOTT-122a at 298 and 273 K in the pressure range 0 − 100 kPa. The simulated CH_4 isotherms of NOTT-122a show excellent agreement with the experimental isotherms.

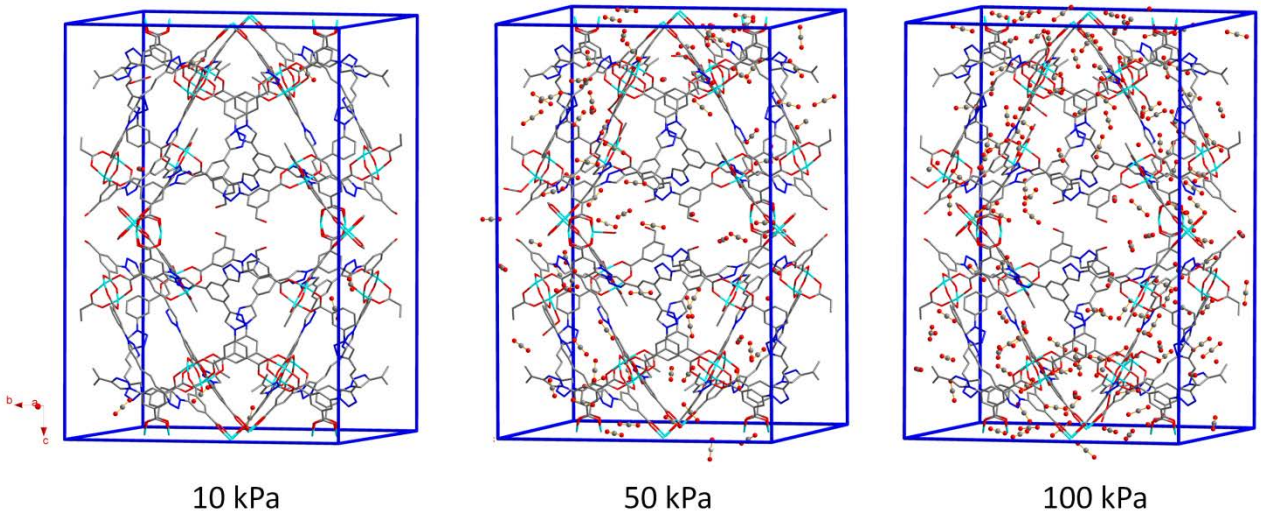

Figure S25. Adsorption of CO_2 into the structure of NOTT-122a containing hierarchically-assembled cages derived from GCMC simulations at different pressures and 273 K.

References:

1. Cadeddu, A.; Ciesielski, A.; Malah, T. E.; Hecht, S.; Samorì, P. *Chem. Commun.* **2011**, *47*, 10578–10580.
2. Chan, T. R.; Hilgraf, R.; Sharpless, K. B.; Fokin, V. V. *Org. Lett.* **2004**, *6*, 2853−2855.
3. Sheldrick, G. M. *SHELXS*97. *Acta Crystallogr., Sect. A* **2008**, *64*, 112–122.
4. Spek, A. L. *Acta Crystallogr., Sect. D*, **2009**, *65*, 148–155.
5. Czepirski, L.; Jagiello, J. *Chem. Eng. Sci.* **1989**, *44*, 797–801.
6. Jagiello, J.; Bandosz, T. J.; Schwarz, J. A. *Langmuir* **1996**, *12*, 2837–2842.
7. Anson, A.; Jagiello, J.; Parra, J. B.; Sanjuan, M. L.; Benito, A. M.; Maser, W. K.; Martinez, M. T. *J. Phys. Chem. B* **2004**, *108*, 15820–15826.
8. Download, instructions, and further details on the use and capabilities of this software package are available online at http://www.r-project.org.
9. O'Koye, I. P.; Benham, M.; Thomas, K. M. *Langmuir* **1997**, *13*, 4054–4059.
10. Reid, C. R.; O'Koye, I. P.; Thomas, K. M. *Langmuir* **1998**, *14*, 2415–2425.
11. Reid, C. R.; Thomas, K. M. *Langmuir* **1999**, *15*, 3206–3218.

12. Zheng, B.; Bai, J.; Duan, J.; Wojtas, L.; Zaworotko, M. J. *J. Am. Chem. Soc.* **2011**, *133*, 748–751.

13. Potoff, J. J.; Siepmann, J.I. *AIChE Journal* **2002**, *47*, 1676−1682.

14. Peng, D.-Y.; Robinson, D. B. *Ind. Eng. Chem. Fundamen.* **1976**, *15*, 59–64.

15. Rappe, A. K.; Casewit, C. J.; Colwell, K. S.; Goddard III, W. A.; Skid, W. M. *J. Am. Chem. Soc.* **1992**, *114*, 10024−10035.

16. Panda, T.; Pachfule, P.; Chen,Y.; Jiang, J.; Banerjee, R. *Chem. Commun.* **2011**, *47*, 2011−2013.

17. Garberoglio, G.; Skoulidas, A. I.; Johnson, J. K. *J. Phys. Chem. B.* **2005**, *109*, 13094−13103.

18. Skoulidas, A. I.; Sholl, D. S. *J. Phys. Chem. B.* **2005**, *109*, 15760–15768.

19. Babarao, R.; Jiang, J. W. *Langmuir* **2008**, *24*, 6270−6278.

20. Mayo, S. L.; Olafson, B. D.; Goddard III, W. A. *J. Phys. Chem.* **1990**, *94*, 8897−8909.

21. Shao, Y. et al. *Phys. Chem. Chem. Phys.* **2006**, *8*, 3172.

22. Gupta, A.; Chempath, S.; Sanborn, M. J.; Clark, L. A.; Snurr, R. Q. *Mol. Simul.* **2003**, *29*, 29–46.